4-18-2022

GM1 ganglioside modifies microglial and neuroinflammatory responses to α-synuclein in the rat AAV-A53T α-synuclein model of Parkinson's disease

Jay S Schneider

Garima Singh

Courtney K. Williams

Vikrant Singh

Molecular and Cellular Neuroscience 120 (2022) 103729

Contents lists available at ScienceDirect

Molecular and Cellular Neuroscience

journal homepage: www.elsevier.com/locate/ymcne

GM1 ganglioside modifies microglial and neuroinflammatory responses to α-synuclein in the rat AAV-A53T α-synuclein model of Parkinson's disease

Jay S. Schneider *, Garima Singh, Courtney K. Williams, Vikrant Singh

Department of Pathology, Anatomy and Cell Biology, Thomas Jefferson University, Philadelphia, PA 19107, USA

ARTICLE INFO

Keywords:
α-Synuclein
GM1 ganglioside
Microglia
Neuroinflammation
Parkinson's disease

ABSTRACT

Among the pathological events associated with the dopaminergic neurodegeneration characteristic of Parkinson's disease (PD) are the accumulation of toxic forms of α-synuclein and microglial activation associated with neuroinflammation. Although numerous other processes may participate in the pathogenesis of PD, the two factors mentioned above may play critical roles in the initiation and progression of dopamine neuron degeneration in PD. In this study, we employed a slowly progressing model of PD using adeno-associated virus-mediated expression of human A53T α-synuclein into the substantia nigra on one side of the brain and examined the microglial response in the striatum on the injected side compared to the non-injected (control) side. We further examined the extent to which administration of the neuroprotective ganglioside GM1 influenced α-synuclein-induced glial responses. Changes in a number of microglial morphological measures (i.e., process length, number of endpoints, fractal dimension, lacunarity, density, and cell perimeter) were indicative of the presence of activated microglial and an inflammatory response on the injected side of the brain, compared to the control side. In GM1-treated animals, no significant differences in microglial morphology were observed between the injected and control striata. Follow-up studies showed that mRNA expression for several inflammation-related genes was increased on the A53T α-synuclein injected side vs. the non-injected side in saline-treated animals and that such changes were not observed in GM1-treated animals. These data show that inhibition of microglial activation and potentially damaging neuroinflammation by GM1 ganglioside administration may be among the many factors that contribute to the neuroprotective effects of GM1 in this model and possibly in human PD.

1. Introduction

The mechanisms leading to the initiation and perpetuation of substantia nigra (SN) dopamine (DA) neuron degeneration in Parkinson's disease (PD) are still not completely known. Mitochondrial dysfunction, oxidative stress, free radical generation, genetic mutations, neurochemical imbalances, defects in ganglioside synthesis and catabolism, reduced neurotrophic support and/or combinations of these as well as a number of other factors have been proposed as underlying or contributing to the neuropathology of PD (ex., Ferreira and Massano, 2017; Hadaczek et al., 2015; Ho et al., 1996; Jenner, 1991; Schapira et al., 1990; Schapira et al., 1998; Schneider, 2021; Tomac et al., 1995). Additionally, activated microglia and neuroinflammation, may play an important role in DA neuron degeneration in the PD brain. Human leukocyte antigen-DR (HLA-DR) positive microglia (McGeer et al., 1988) have been found in the SN of idiopathic PD patients as well as in patients with 1-methyl-4-phenyl-1,2,3,6-tetrahydropyridine (MPTP)-induced parkinsonism, even years after the original toxin exposure (Langston et al., 1999). Since these early reports, there are now several additional lines of evidence that support the idea that activation of microglia, with subsequent production of pro-inflammatory cytokines, such as tumor necrosis factor-alpha (TNF-alpha) and interleukin-1 beta (IL-1 beta), plays an important role in the progression of PD pathology (Gerhard et al., 2006; Mogi et al., 1994; Ouchi et al., 2005; Sanchez-Guajardo et al., 2010; Zhang et al., 2017).

Preclinical studies have examined the potential role of microglia and inflammation in DA neuron degeneration in toxin-induced models of PD (Du et al., 2001; Furuya et al., 2004; He et al., 2001; Kurkowska-Jastrzebska et al., 1999; LaVoie et al., 2004; Wu et al., 2002) and α-synuclein (α-Syn) may play an important role in this process. Accumulating evidence from various studies also suggests a relationship between α-Syn oligomerization, generation of reactive oxygen species, oxidative stress,

* Corresponding author at: Department of Pathology, Anatomy and Cell Biology, Thomas Jefferson University, 1020 Locust Street, 521 JAH, Philadelphia, PA 19107, USA.
E-mail address: jay.schneider@jefferson.edu (J.S. Schneider).

https://doi.org/10.1016/j.mcn.2022.103729
Received 9 February 2022; Received in revised form 22 March 2022; Accepted 12 April 2022
Available online 18 April 2022

and neuroinflammation via activation of microglial cells (Rocha et al., 2018; Wang et al., 2016; Zhang et al., 2007; Zhang et al., 2005). Accumulation of wild-type and mutated forms of α-synuclein (i.e., A30P, A53T) lead to elevated microglia-related ROS production (Ostrerova-Golts et al., 2000; Rocha et al., 2018; Wang et al., 2016; Zhang et al., 2007). Accumulation of wild-type α-Syn in a rAAV model showed that enhanced α-Syn expression not only leads to persistent microglia activation, but that the degree of SN neuropathology induced by α-Syn influences the type of microglial response that occurs (Sanchez-Guajardo et al., 2010). For example, α-Syn expression at a level that induced significant SN DA cell death resulted in the chronic induction of CD68-expressing macrophagic microglia (Sanchez-Guajardo et al., 2010). Despite the evidence supporting a role of microglial activation and/or neuroinflammatory changes in PD pathology, clinical trials using anti-inflammatory therapies have not been successful in slowing the progression of PD (Hung and Schwarzschild, 2020).

We recently reported that treatment with the glycosphingolipid GM1 ganglioside was neuroprotective in an AAV A53T α-Syn model in the rat (Schneider et al., 2019). Treatment with GM1 ganglioside had beneficial effects on striatal DA levels and behavior, protected SNc DA neurons from degeneration, and appeared to decrease the amount of aggregated α-Syn (Schneider et al., 2019). Gangliosides are sialic acid containing glycosphingolipids of which the major species in brain are a- and b-series gangliosides GM1, GD1a, GD1b, and GT1b. Gangliosides expressed by neurons and other cell types in brain serve critically important physiological functions and GM1, a major component of membrane signaling domains, plays an important role in variety of process that could be potentially neuroprotective or disease modifying in PD including, interacting with a variety of proteins that modulate ion transport, G protein-coupled receptors (GPCRs), immune system reactivity, and neuroprotective signaling (Ledeen and Wu, 2015; Schneider, 2021). Considering the previous data showing neuroprotection from α-Syn toxicity with GM1 administration, potential anti-inflammatory effects of GM1, and the knowledge that microglia morphology and function are closely related (Fernandez-Arjona et al., 2017), the present study was conducted to investigate the extent to which GM1 administration in the rat AAV a53T α-Syn model could modulate microglial morphological characteristics and potentially, neuroinflammatory processes.

2. Materials and methods

2.1. Animals and vector delivery

The vector used in this study (GeneDetect Ltd., Auckland, New Zealand) has been described in detail previously (Koprich et al., 2011; Schneider et al., 2019). Briefly, a chimeric adeno-associated vector (AAV) of a 1/2 serotype (capsid expresses AAV1 and AAV2 serotype proteins in a 1:1 ratio) with human A53T α-Syn expression driven by a chicken beta actin (CBA) promoter hybridized with the cytomegalovirus (CMV) immediate early enhancer sequence was used. A woodchuck post-transcriptional regulatory element (WPRE) and a bovine growth hormone polyadenylation sequence (bGH-polyA) were also incorporated to further enhance transcription following transduction.

All animal procedures were approved by the Thomas Jefferson University Institutional Animal Care and Use Committee and conducted in accordance with the National Institutes of Health Guide for the Care and Use of Laboratory Animals. Adult male Sprague-Dawley rats (280 to 300 g, Envigo), were housed three to a cage with ad libitum access to food and water during a 12-hour light/dark cycle. All surgeries were performed under general isoflurane anesthesia. Once fully anesthetized, animals were placed in a Kopf stereotaxic frame with the incisor bar set to achieve a flat skull position. A small incision was made along the midline of the scalp and a small hole was drilled over the SN (coordinates AP: −5.3, L: 2.2, D: 7.5 below skull) on one side and a 36 gauge needle attached to a Hamilton syringe loaded with AAV-A53T-synuclein (2.55×10^{12} GP/ml) was slowly lowered into the brain and 2.0 μl was injected at a rate of 0.2 μl/min. The needle was slowly withdrawn following a 5 min wait period after completion of the injection, the skin wound was closed, post-surgery analgesia (meloxicam 1 mg/kg) was administered, and the animal was transferred to a recovery cage.

Rats were randomly assigned to receive either daily GM1 ganglioside (porcine brain derived GM1, 30 mg/kg, i.p., Qilu Pharmaceutical Co., Ltd.) injections or similar volume saline injections for 4 weeks, beginning 24 h after AAV-A53T-synuclein surgery. The dose of 30 mg/kg was selected based on the previously observed positive response of this model to GM1 ganglioside (Schneider et al., 2019).

2.2. Behavioral testing

Forelimb use was analyzed using the cylinder test, as previously described (Schneider et al., 2019). Briefly, an animal is placed in a clear 33 cm × 50 cm Plexiglass cylinder located in a dimly lit room in front of a mirror in order to visualize limb use from all angles. The paw contralateral to the side of the AAV-A53T-α-synuclein injection was marked prior to the start of each test session. Forelimb use was assessed over a 10 min observation period by scoring twenty observations of weight-bearing paw placements on the cylinder wall with the ipsilateral, contralateral (relative to the AAV-A53T-α-synuclein-injected side), and both paws. Percent ipsilateral (ipsi) and contralateral (contra) paw touches were calculated as [(ipsi + 1/2 both) / total # observations] * 100 and [(contra + 1/2 both) / total # observations] * 100, respectively. Testing occurred prior to surgery (baseline) and at 2 and 4 weeks of GM1 or saline treatment.

2.3. Western blotting

For immunoblotting studies, animals were deeply anesthetized and transcardially perfused with cold PBS to remove blood from the brain. Fresh brains were rapidly removed, sectioned in a chilled rat brain matrix, and SN tissue from control and α-Syn-injected sides of the brain was dissected from 1 mm thick brain sections placed on a chilled dissection plate, and samples were immediately frozen on dry ice for later analyses. Dissected SN samples were homogenized in cold RIPA buffer supplemented with protease and phosphatase inhibitor mix (Halt Protease and Phosphatase Inhibitor Cocktail, Thermo) using a micropestle and then were briefly sonicated. Tissue lysates were then incubated at 4 °C with gentle rotation for 30 min and centrifuged at 13,000 rpm, 4 °C for 15 min in a refrigerated microcentrifuge. The supernatant was then removed and aliquoted into fresh tubes and immediately frozen on dry ice and stored at −80 °C. An aliquot of the supernatant was used to determine the protein concentration of the lysate using a Micro BCA Assay Kit (Thermo) according to the manufacturer's protocol. Prior to performing western blotting to evaluate the amount of Iba1 in tissue lysates, the linear range of signal detection and quantitation for Iba1 and β-Actin (housekeeping control) was determined using control SN tissue lysates. Next, 17 μg of SN tissue lysate was mixed with LDS sample buffer (1× final, GenScript) plus β-mercaptoethanol (Sigma-Aldrich), denatured at 70 °C for 10 min and resolved on a 4–20% SurePAGE Bis-Tris precast gel using MES running buffer (GeneScript). Resolved proteins were transferred to an activated PVDF membrane (0.2 μ PVDF membrane, Millipore) using Transfer buffer (GenScript) containing 10% Methanol (Fisher Scientific) in an XCell II blot module (Invitrogen). After protein transfer, the membrane blot was cut into strips, according to the molecular weight of the proteins analyzed, and blocked in 2.5% Non-Fat Dry Milk solution (Cell Signaling) in TBS containing 0.05% Tween-20 (TBS-T). Blots were incubated overnight with anti-Iba1 antibody (Abcam, Cat# ab178846, RRID: AB_2636859, 1:3000 dilution) or anti β-Actin antibody (Proteintech, Cat# 66009-1, RRID: AB_2687938, 1:5000 dilution) at 4 °C with gentle shaking. After washing with TBS-T, blots were incubated with HRP-labeled anti-rabbit or anti-mouse secondary antibodies (Cell Signaling Technology, Cat# 7074, RRID:

AB_2099233; Cat# 7076, RRID: AB_330924, 1:10,000 dilution each) for 1 h at RT with gentle shaking. The blots were then washed in TBS-T and developed using Immobilon ECL Ultra (Millipore) for anti-Iba1 blots and Immobilon Western Chemiluminescent Substrate (Millipore) for anti-β-Actin blots. The chemiluminiscence signal was imaged using a FluoRChem M system (ProteinSimple) and the images were exported to Image Studio Lite (Version 5.2, LI-COR) software for densitometric analysis of signal bands. The Iba1 signal was normalized to the β-Actin signal for each sample and normalized Iba1 signal from the α-Syn injected side was expressed as a percentage of the signal from the non-injected side.

2.4. Immunohistochemistry and microglial analyses

Animals were deeply anesthetized and transcardially perfused with cold PBS followed by cold 4% paraformaldehyde in PBS. Fixed tissue blocks were immersed in 30% sucrose for cryoprotection and sectioned frozen on a sliding microtome. Striatal tissue was sectioned (30 μm section thickness) and free-floating sections were processed for immunohistochemistry. Endogenous peroxidase activity was quenched using 3% hydrogen peroxide in PBS containing 0.1% Tween-20 (PBS/T) followed by blocking in PBS/T containing 10% normal goat serum and 2% BSA. Sections were then incubated overnight in Iba1 (Ionized calcium Binding Adapter molecule 1) primary antibody (rabbit anti-Iba1, 1:5000, EnCor Biotechnology, Inc., Cat# RPCA-IBA1, RRID: AB_2722747), followed by incubations in biotinylated secondary antibody (goat-anti-rabbit 1:400, VECTOR Laboratories, Inc., Cat# BA-1000-1.5), avidin biotin complex (VECTASTAIN Elite ABC system, VECTOR Laboratories), and visualization of reaction product using 3,3-diaminobenzidine (DAB) (Immpact DAB, VECTOR Laboratories). Sections were then mounted, dehydrated, cleared and coverslipped. Some sections were processed, using the same methods described above, for visualization (or absence) of α-Syn using a mouse anti-α-Syn primary antibody (clone 211; 1:2000, Millipore, Cat# 36-008) and biotinylated goat-anti-mouse secondary (1:2000, VECTOR Laboratories, Inc., Cat# BA-9200).

Microglial morphological analyses to quantify process lengths and to obtain the number of process endpoints were performed using Fiji (ImageJ) software (RRID: SCR_002285), freely downloadable from https://imagej.net/Fiji, and the Analyze Skeleton (2D/3D) plugin (Young and Morrison, 2018). All slides were coded and all analyses were performed with the experimenter blinded to animal identification and treatment group. The skeleton analysis was performed on brightfield images of distinct microglial cells captured using a Nikon Eclipse *Ni* microscope (20× objective) and NIS-Elements software according to methods described in detail by Young and Morrison (Young and Morrison, 2018). Briefly, 8-bit images of randomly selected microglia cells from control (non-injected hemisphere) and α-Syn injected hemispheres from up to 4 sections through the striatum per animal were collected and converted to skeletonized images by applying an FFT Bandpass Filter to remove noise, converting images to grayscale, adjusting brightness/contrast to optimize visualization of microglia processes, applying an Unsharp Mask filter to further increase contrast, performing a despeckle step to reduce noise, converting the image to binary and further reducing noise by applying additional despeckle and Remove Outliers steps. The optimized binary image was saved and then skeletonized and analyzed using the Analyze Skeleton plugin with the Branch Information box checked (Young and Morrison, 2018). Results and branch information were copied and trimmed (Young and Morrison, 2018) and the total number of endpoints collected from each microglia image were calculated along with the summed length of all branches collected from each microglia image.

Next, fractal analysis of microglia was run using the FracLac plugin, *FracLac for ImageJ* (available at the ImageJ website, National Institutes of Health) according to methods described in detail elsewhere (Fernandez-Arjona et al., 2017; Young and Morrison, 2018). Briefly, the rectangle tool was used to create a region of interest (ROI) large enough to capture an entire microglial cell image consistently for each cell to be analyzed from previously collected binary skeletonized images. The binary images of microglia randomly selected for fractal analysis were converted to an outline using the Binary/Outline tool and Fractal Analysis/FracLac was opened from the plugin toolbar. Once opened, box counting (BC) was selected from the FracLac menu (grid design Num G set to 4), convex hull and bounding circle panel was selected and options boxes metrics, bounding circles, and convex hull were selected. Each image was then scanned by selecting the Scan button to run a box-counting scan on the selected image (Young and Morrison, 2018). Density, span ratio, perimeter, and circularity data were extracted from the Hull and Circle Results file; fractal dimension and lacunarity data were extracted from the Box Count Summary Results file (Fernandez-Arjona et al., 2017; Young and Morrison, 2018).

2.5. mRNA expression of neuroinflammatory-related genes

The following genes were chosen for analysis, based on their purported roles in various neuroinflammatory processes: interleukin 1 beta (IL-1β), interleukin 6 (IL-6), tumor necrosis factor alpha (TNFα), interleukin 10 (IL-10), orphan nuclear receptor Nurr1, NLR family pyrin domain containing 3 (NLRP3) inflammasome; Cathepsin D (CTSD), nitric oxide synthase 2 (NOS2), and prostaglandin-endoperoxide synthase 2 (PTGS2). These particular genes have been associated with the neurodegenerative process in PD, the response to α-Syn toxicity, microglial inflammatory responses, anti-inflammatory tissue responses, and/or neuroprotection (Su et al., 2008; Rocha et al., 2018; Chung et al., 2009; Lobo-Silva et al., 2016; Gordon et al., 2018).

RNA was extracted from fresh frozen SN samples using Zymo Directzol RNA miniprep Plus. cDNA was prepared using Qiagen Omniscript RT and qPCR was carried out using SYBR Green and commercially sourced primers from Qiagen against genes described above: IL-1β (Catalog No. PPR06480B-200), IL-6 (Catalog No. PPR06483B-200), IL-10 (Catalog No. PPR06479A-200), Nurr1 (Catalog No. PPR52704F-200), NLRP3 (Catalog No. PPR56639A-200), CTSD (Catalog No. PPR45222A-200), NOS2 (Catalog No. PPR44835A-200), PTGS2 (Catalog No. PPR49747F-200) on a Roche LightCycler 480 II. To confirm specificity of amplification the products were subjected to a melting curve analysis at the end of the final annealing period. The ΔΔCt method was used to calculate mRNA expression change relative to *GAPDH* (housekeeping gene) expression.

2.6. Statistical analyses

All statistics were performed using GraphPad Prism software (v9). Microglial morphological parameters obtained from cells on the control and α-Syn-injected sides of the brain in saline control and GM1-treated animals were compared using two-way analysis of variance followed by post hoc comparisons using Tukey's multiple comparisons test. Immunoblotting data and gene expression data were compared by one-way analysis of variance, also followed by post hoc pair-wise comparisons using Bonferroni's multiple comparison test. Cylinder test data were compared using paired *t*-tests. All analyses were two-sided and statistical significance was set at $P < 0.05$.

3. Results

3.1. Alpha-synuclein and GM1 effects on motor behavior

The cylinder test was used to assess spontaneous forelimb use in AAV-A53T α-Syn-transduced animals. Animals that received AAV-A53T α-Syn followed by administration of saline or GM1 daily for 2 weeks all developed a significant asymmetry in paw use with preference for making contact with the cylinder with ipsilateral forepaw relative to the side of virus injection (mean ± SEM: baseline/saline: 51.0 ± 2.5%; 2

weeks/saline: 63.8 ± 2.9%, baseline/GM1: 48.0 ± 2.4%; 2 weeks/GM1: 71.0 ± 3.4). There was no significant difference between the saline and GM1-treated animals in percent of ipsilateral paw use at 2 weeks (Fig. 1A). At the 4 week point, animals receiving daily saline injections had increased ipsilateral paw usage compared to 2 weeks whereas animals receiving daily GM1 injections had a decrease in ipsilateral paw usage compared with 2 weeks and the difference between percent of ipsilateral paw use between saline and GM1-treated animals was significant at the 4 week time point (mean ± SEM: baseline/saline: 51.0 ± 2.5%; 4 weeks/saline: 77.0 ± 5.1%, baseline/GM1: 48.0 ± 2.4%; 4 weeks/GM1: 65.0 ± 2.9; Fig. 1B).

3.2. Alpha-synuclein and GM1 effects on Iba1 protein levels

Iba1 expression was assessed in the SN lysates 2 weeks and 4 weeks after unilateral AAV-A53T α-Syn injection and was expressed as a percent of the expression on the control side of the brain for each animal (Fig. 2). At 2 weeks, Iba1 expression on the injected side was 163.2 ± 16.1% of that measured on the control, non-injected side in saline-treated animals. The level of expression of Iba1 was similar in animals that received 2 weeks of GM1 administration (149.6 ± 9.1% on the injected side relative to the control side). At 4 weeks post AAV-A53T α-Syn injection, Iba1 expression on the injected side was 178.7 ± 31.0% of that on the non-injected side in saline-treated animals but only 118.7 ± 13.8% on the injected side vs. the non-injected side in GM1-treated animals ($P < 0.05$).

3.3. Alpha-synuclein and GM1 effects on microglial morphology

As effects of GM1 administration on Iba1 protein levels in the SN were not significant at the 2 week time point, analyses of effects of α-Syn and potentially modulatory effects of GM1 on microglia morphology were assessed only at the 4 week time point, when significant behavioral effects and effects on Iba1 levels in GM1-treated animals were observed. The α-Syn accumulation in the striatum on the injected side, and absence on the non-injected side, was confirmed in all animals (Fig. 3).

In the normal, healthy condition, microglia are mostly characterized by a ramified morphology whereas after injury or in the case of neuroinflammation, microglia are characterized as having shorter, thicker processes (Fernandez-Arjona et al., 2017). The number of process endpoints (an indication of the extent of process ramification) (Young and Morrison, 2018) were quantified from photomicrographs of Iba1-stained microglia in the striatum (control side and α-Syn injected side) of α-Syn/saline and α-Syn/GM1-treated animals. Following 4 weeks of saline administration after AAV A53T α-Syn injection into the SN, there was a significant main effect of α-Syn ($F_{(1, 116)} = 30.03$, $P < 0.0001$), a significant main effect of treatment ($F_{(1, 116)} = 13.64$, $P = 0.0003$), and a significant interaction effect ($F_{(1, 116)} = 4.82$, $P = 0.0303$), with a decrease in the number of endpoints per microglial cell in the striatum on the α-Syn-injected side of the brain (mean 46.8 ± 3.3) compared to the control side (mean 76.3 ± 4.5; control side/saline vs. α-Syn side/saline $P < 0.0001$). In comparison, there was no significant difference in the number of endpoints per microglial cell in the striatum on the α-Syn-injected side compared to the control side in animals that received 4 weeks of GM1 administration (Fig. 4A). Process length/cell, an additional measure of microglial process ramification was also assessed. Similar to what was observed for process endpoints, there was a significant main effect of α-Syn ($F_{(1, 116)} = 31.10$, $P < 0.0001$), a significant main effect of treatment ($F_{(1, 116)} = 28.04$, $P < 0.0001$), and a significant interaction effect ($F_{(1, 116)} = 4.37$, $P = 0.0388$), with a decrease in

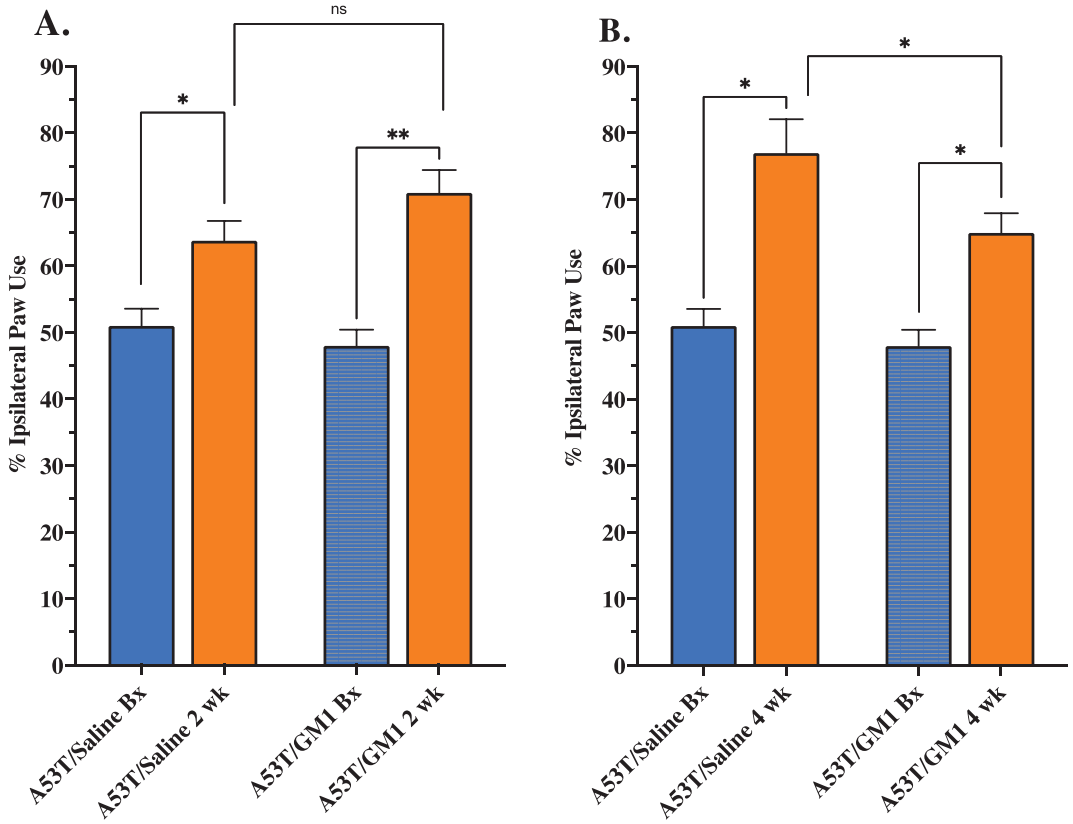

Fig. 1. Effect of GM1 on spontaneous forelimb use. (A) At 2 weeks following AAV-A53T α-synuclein injection, saline-treated animals (N = 5) favored the use of the limb ipsilateral to the injection and this response was also observed in GM1-treated animals (N = 5). There was no significant difference between percent of ipsilateral paw use between saline and GM1-treated animals at 2 weeks. (B) At 4 weeks, use of the limb ipsilateral to the injection was favored to a greater extent than it was at 2 weeks in saline-treated animals (N = 5), but with continued GM1 use, this response was reduced at 4 weeks, resulting in a significant difference between ipsilateral paw use in saline and GM1-treated animals (N = 5). *$P < 0.05$ vs. baseline; *$P < 0.05$ 4 week saline vs. 4 week GM1; **$P < 0.01$ vs. baseline.

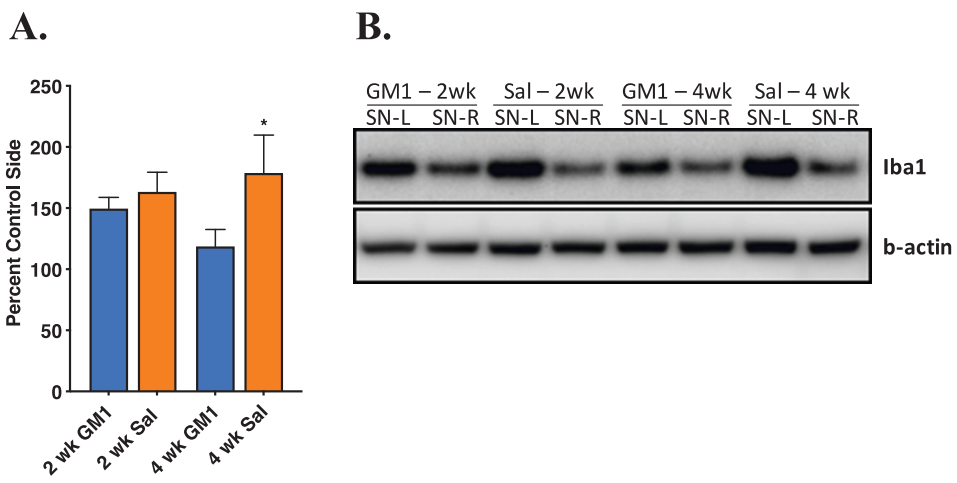

Fig. 2. GM1 treatment significantly affected Iba1 levels in the substantia nigra (SN) at 4 weeks but not at 2 weeks after AAV-A53T injection into the SN. (A) Western blot results (mean ± SEM) are presented as Iba1 expression on the side of α-synuclein injection as a percent of the expression level on the contralateral (control, non-injected) side. There was a significant difference in Iba1 expression between animals that received 4 weeks of saline injections and those that received 4 weeks of GM1 injections, with a decrease in Iba1 expression in GM1-treated animals (N = 5/group, $^*P < 0.05$). (B) Representative Western blots from 2 week and 4 week animals showing a minimal response to GM1 on Iba1 expression at 2 weeks and a significant decrease in Iba1 expression in the SN after 4 weeks of GM1 treatment. Data are shown for SN-L (side of AAV-A53T injection) and SN-R (control, non-injected side) from the same animal following 2 or 4 weeks of GM1 or saline (Sal) administration. Beta-actin was used as loading control.

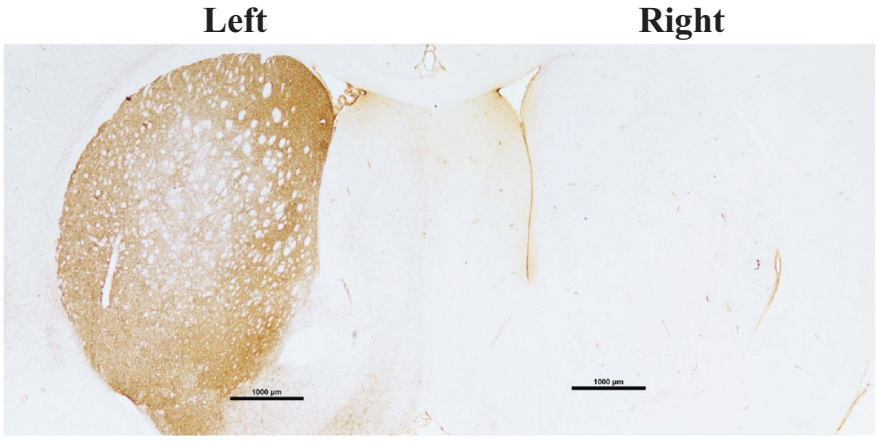

Fig. 3. Immunohistochemical staining of α-synuclein on the side injected with AAV-A53T α-synuclein (left), and the absence of staining on the uninjected control side (right), four weeks post surgery.

process lengths per microglial cell in the striatum on the α-Syn-injected side of the brain compared to the control side (control side/saline (mean 513.2 ± 27.3 µm vs. α-Syn side/saline (mean 329.1 ± 22.3 µm, $P < 0.0001$). In comparison, there was no statistically significant difference in process lengths of microglial cells on the α-Syn-injected side (mean 506.5 ± 23.6 µm) compared to the control side (mean 590.2 ± 22.5) in animals that received 4 weeks of GM1 administration (Fig. 4B).

Additional morphological parameters were analyzed to try to gain additional insight to the effects of both α-Syn and GM1 administration on microglial responses. There were distinct differences in morphological profiles of microglia on the α-Syn-injected side in the striatum in saline control (Fig. 5) compared to GM1-treated animals (Fig. 6). An increase in density is taken to show the tendency of microglial cells to become more compact in response to an injury signal (Fernandez-Arjona et al., 2017). When density was analyzed, there was a significant main effect of α-Syn ($F_{(1, 56)} = 4.37$, $P = 0.0413$) with a significant increase in this parameter on the α-Syn-injected side (mean 0.035 ± 0.001) compared to the control side (mean 0.041 ± 0.002) in saline-treated animals ($P = 0.0049$) (Fig. 7A). In comparison, there was no statistically significant difference between the density measures on the control and α-Syn-injected sides in the GM1-treated animals (Fig. 7A). The increase in density of microglial cells on the α-Syn-injected side in the saline control animals indicates the tendency for these cells to become more compact due to increased α-Syn expression, a microglial response not seen in the GM1-treated animals.

Fractal dimension, which can identify microglial forms ranging from rounded to complex branched (Fernandez-Arjona et al., 2017) was measured and showed a significant effect of α-Syn ($F_{(1, 56)} = 19.46$, $P < 0.0001$), a significant effect of treatment ($F_{(1, 56)} = 6.46$, $P = 0.0138$) and a significant interaction effect ($F_{(1, 56)} = 10.63$, $P < 0.0001$). There was a significant decrease in the fractal dimension measure on the α-Syn-injected side (mean 1.29 ± 0.01) compared to the control side (mean 1.39 ± 0.01) in saline-treated animals ($P < 0.0001$) (Fig. 7B). In comparison, there was no statistically significant difference between the fractal dimension measures on the control (mean 1.38 ± 0.01) and α-Syn-injected sides (mean 1.37 ± 0.01) in the GM1-treated animals (Fig. 7B). The reduction in fractal dimension on the α-Syn-injected side in the saline control animals indicates a lesser degree of pattern (branch) complexity of microglial cells that was not observed on the α-Syn-injected side in the GM1-treated animals.

Cell circularity (the value of a circle is 1, the value of a linear polygon is 0) was measured and there was no significant effect of α-Syn ($F_{(1, 56)} = 1.633$, $P = 0.2065$) and no significant treatment effect was detected on this parameter ($F_{(1, 56)} = 3.057$, $P = 0.0859$). There were no significant differences in this parameter on control versus α-Syn-injected sides of the brain in saline-treated animals nor in the GM1-treated animals

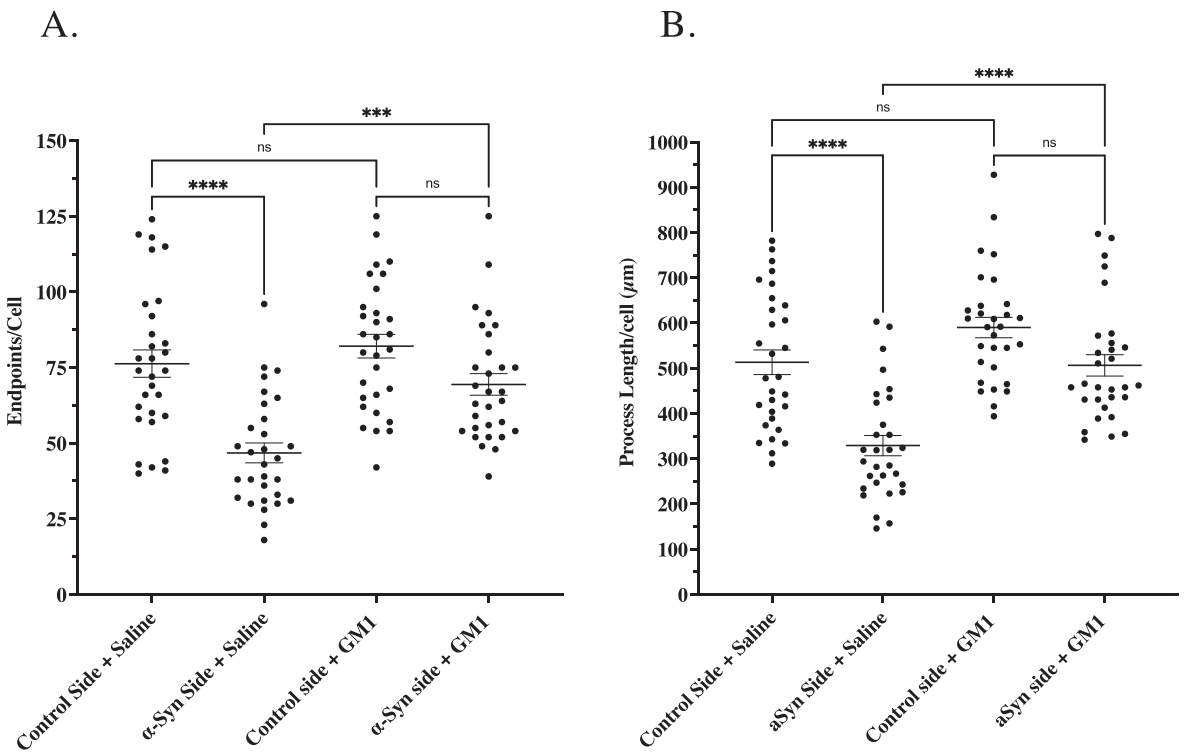

Fig. 4. Microglial cell ramifications are altered by α-synuclein toxicity and further modified by GM1 administration. At 4 weeks after AAV-A53T injection in to the SN, microglial activation in the striatum on the injected side (aSyn side) coincided with a significant decrease in cell ramifications, resulting in a significant decrease in process length per cell (A) and number of endpoints per cell (B), in comparison to the same measure taken from microglia from the non-α-synuclein injected side of the brain (Control side). GM1 treatment, initiated 24 h after AAV-A53T injection in the SN and administered daily for 4 weeks, resulted in no significant differences in process lengths or number of endpoints in the a-Syn injected side of the brain compared to the same measures from the Control side of the brain. There was a significant difference in these measures between the aSyn side in saline-treated animals compared to the aSyn side in the GM1-treated animals (N = 5 animals per treatment group, 6 cells randomly selected from α-Syn and control sides and analyzed in each animal; ****$P < 0.0001$ Control side-Saline vs. aSyn side-Saline; ****$P < 0.0001$ aSyn side-Saline vs. aSyn side + GM1; ***$P = 0.0003$ a-Syn side-Saline vs. aSyn side + GM1).

(Fig. 7C).

The parameter of lacunarity measures heterogeneity or invariance in shape. A low lacunarity value implies homogeneity while a high value implies heterogeneity, with the image containing many differently sized gaps or lacunae (Fernandez-Arjona et al., 2017). There was a significant effect of α-Syn ($F_{(1, 56)} = 4.099$, $P = 0.0477$) and a significant treatment effect on this parameter ($F_{(1, 56)} = 6.147$, $P = 0.0162$). Pairwise comparisons showed a decrease on the α-Syn-injected side (mean 0.39 ± 0.01) compared to the control side (mean 0.43 ± 0.01) in saline-treated animals ($P = 0.045$) (Fig. 7D). In comparison, there was no statistically significant difference between the lacunarity measures on the control (mean 0.44 ± 0.01) and α-Syn-injected sides (mean 0.44 ± 0.02) in the GM1-treated animals (Fig. 7D). Since a lower lacunarity value indicates homogeneity, these data suggest that on the α-Syn-injected side in the saline control animals, but not in the GM1-treated animals, microglia changed toward a more homogeneous shape.

In *FracLac*, the convex hull algorithm measures the size and shape of a binary image. The convex hull span ratio, also known as form factor, is the ratio of the major to the minor axes of the convex hull. There were no significant differences in this parameter between control and α-Syn-injected sides in either saline-treated or GM1-treated animals (Fig. 7E).

Cell perimeter was measured based on the single outline cell shape (Fernandez-Arjona et al., 2017). A more compact shape is associated with a lower cell perimeter measure. There was a significant effect of α-Syn ($F_{(1, 56)} = 13.85$, $P = 0.0005$), a significant treatment effect ($F_{(1,56)} = 14.42$, $P = 0.0004$) and a significant interaction effect ($F_{(1, 56)} = 4.978$, $P = 0.0297$) on this parameter. Pairwise comparisons showed a significant decrease on the α-Syn-injected side (mean 1575.0 ± 46.5) compared to the control side (mean 1782.0 ± 31.7) in saline-treated animals ($P = 0.0005$) (Fig. 7F). In comparison, there was no statistically significant difference between the perimeter measures on the control (mean 1837.0 ± 30.0) and α-Syn-injected sides (mean 1785.0 ± 29.4) in the GM1-treated animals (Fig. 7F).

3.4. Changes in expression of neuroinflammatory-related genes

There was a significant treatment effect in favor of GM1 for IL-6 ($F_{(3,30)} = 36.64$, $P < 0.0001$), IL-10 ($F_{(3,30)} = 43.29$, $P < 0.0001$), and CTSD ($F_{(3,30)} = 6.036$, $P = 0.0024$) gene expression. Expression of these genes were significantly increased in the SN (data expressed as fold change (±SEM) in left (α-Syn-injected side)/right (control side) ratios) at 4 weeks post surgery in saline-treated animals compared with gene expression levels in animals that received 4 weeks of GM1 administration ($P < 0.0001$ for IL-6 and IL-10; $P < 0.01$ for CTSD) Fig. 8). There was a significant treatment effect in favor of GM1 on TNFα gene expression at 2 weeks post surgery ($F_{(3,29)} = 3.332$, $P = 0.0331$) compared to saline-treated animas ($P < 0.05$), but not at 4 weeks (Fig. 8). Likewise, there was a significant treatment effect in favor of GM1 on NLRP3 gene expression at 2 weeks post surgery ($F_{(3,30)} = 3.173$, $P = 0.0384$) compared to saline-treated animals ($P < 0.05$), but not at 4 weeks (Fig. 8). There were no significant differences in expression IL-1β, Nurr1, PTGS2, or NOS2 in saline or GM1-treated animals at either 2 weeks or 4 weeks (Supplementary Fig. 1).

4. Discussion

Microglial cells can display a diverse range of morphologies and microglial form is linked to microglial function (Karperien et al., 2013). In the normal mature brain, microglia, engaged in essential physiological processes, display a ramified profile and typically present as having

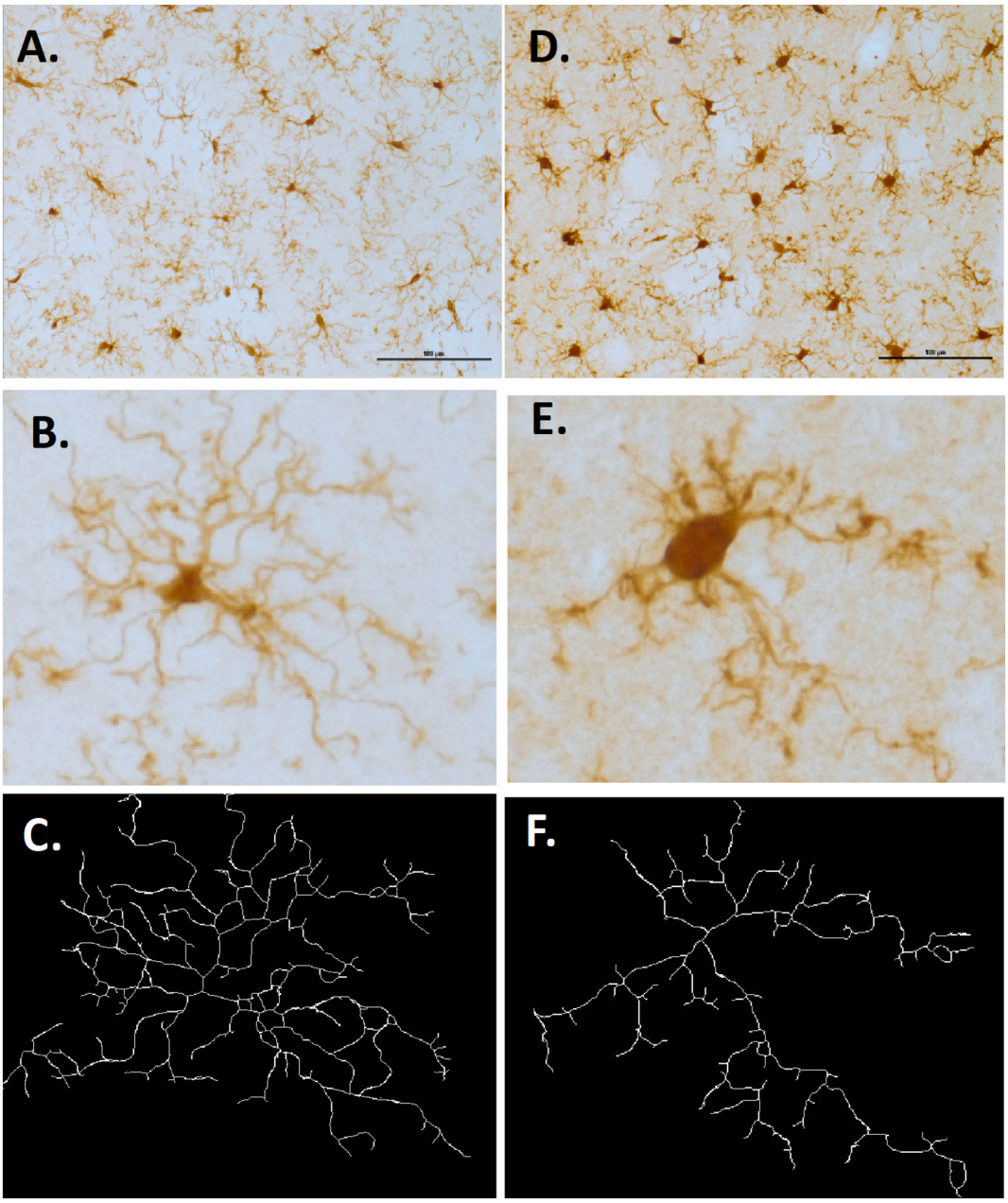

Fig. 5. Photomicrographs of microglial morphological changes in the striatum 4 weeks after AAV-A53T α-synuclein injection into the SN in a saline-control animal. Microglial morphology, evidenced by size and form of the soma and length/branches of process in the striatum on the control (non-injected) side (A and B) was different than observed in the striatum on the injected side of the brain (D and E), showing larger soma and shorter and fewer branches. Corresponding skeleton images of these cells (C and F) further demonstrate the change in morphology associated with α-synuclein toxicity.

a relatively small sized soma and long, "spider-like" processes (Karperien et al., 2013). In response to injury, microglia adopt an unramified form typically considered to be "activated" or "reactive", in which the soma is relatively large and processes are decreased in number and complexity. These latter types of microglia are associated with expression of pro-inflammatory proteins (Karperien et al., 2013). In the present study, we quantified microglial morphology in sections from the striatum in animals that received AAV-A53T-α-Syn injection into the SN on one side of the brain. We describe for the first time, using ImageJ (Fiji) skeleton and fractal analysis (Morrison et al., 2017; Young and Morrison, 2018), morphological changes in striatal microglia in response to α-Syn toxicity, consistent with a neuroinflammatory response, and the attenuation of this glial response by treatment of animals with the neuroprotective ganglioside GM1.

Evidence suggests that phosphorylation and aggregation of α-Syn are involved in the neurodegenerative process in PD, and that the response to α-Syn toxicity involves a variety of cellular processes, including adverse effects on mitochondrial function and activation of microglia (Rocha et al., 2018). The microglial response to toxic α-Syn is complex. For example, activated microglia can engulf extracellular α-Syn and clear it from the extracellular space (either to remove potentially toxic α-Syn derived from dead or dying cells or to remove extracellular/exosomal α-Syn released from intact cells) and the internalization of α-Syn into microglia involves GM1 ganglioside (Park et al., 2009). Studies have shown that GM1 on the cell surface mediates internalization of α-Syn into microglia (Park et al., 2009): depletion of cell surface gangliosides by treatment with the glucosylceramide synthase inhibitor DL-threo-1-phenyl-2-decanoylamino-3-morpholino-1-propanol (PDMP)

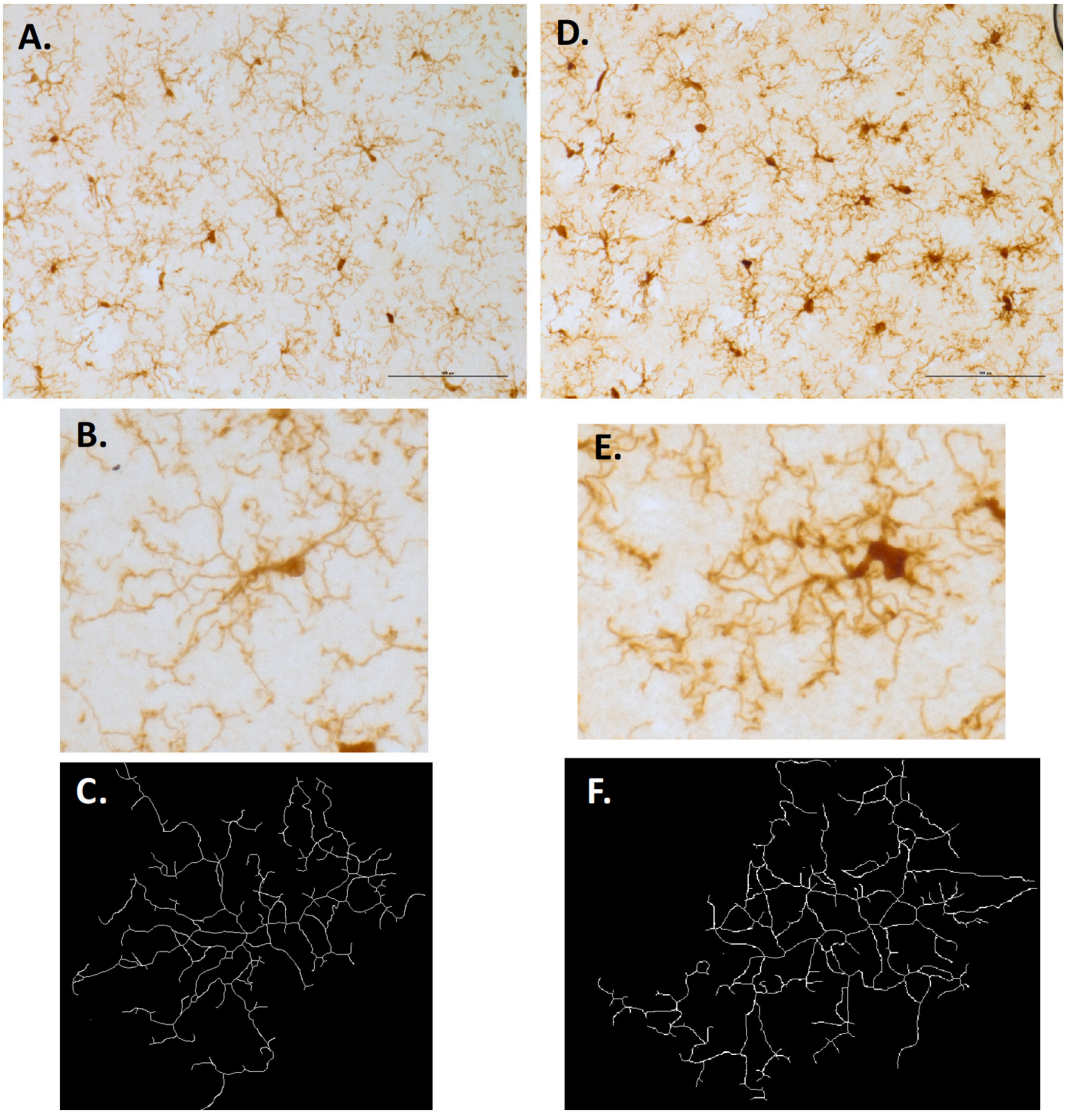

Fig. 6. Photomicrographs of microglial morphological changes in the striatum 4 weeks after AAV-A53T α-synuclein injection into the SN in a GM1-treated animal. While differences in microglial morphology, evidenced by size and form of the soma and length/branches of process in the striatum on the control (non-injected) side (A and B) vs. the injected side (D and E) could still be observed, there was a trend toward normalization of glial morphology in the GM1-treated animals compared to the saline-control animals in Fig. 4. Corresponding skeleton images of these cells (C and F) show that the differences in microglial morphology between the α-synuclein-injected (F) and control sides (C) appear minimal.

inhibited internalization of α-Syn into microglia and this effect was reversed by addition of GM1 (Park et al., 2009). Thus, microglia (and actions of GM1 directly on microglia) may participate in a process that that tries to mitigate α-Syn toxicity and propagation of PD-like neurodegeneration.

Other lines of evidence show early microglial activation in mice over-expressing wild-type α-Syn (Su et al., 2008) and a dose dependent activation of microglia *in vitro* by α-Syn, coincident with increases in production of proinflammatory molecules (Su et al., 2008). Microglial activation and levels of proinflammatory cytokines increase prior to significant levels of α-Syn-mediated neuronal death (Chung et al., 2009; Su et al., 2009; Zhang et al., 2017), and it has been suggested that toxic α-Syn and neuroinflammation may potentiate each other, leading to the degeneration of DAergic neurons (Zhang et al., 2017). Sanchez-Guajardo et al. further demonstrated the complexity of the microglial response in an rAAV α-Syn-based model of PD by showing that distinct activation profiles of microglia, based on expression patterns of CD8 and MCH II, are related to the degree to which α-Syn expression results in cell death (Sanchez-Guajardo et al., 2010). Using a model similar to the one used in our current study, Chung et al. (Chung et al., 2009) reported a neuroinflammatory response in the striatum, characterized by increased levels of Iba-1, activated microglia and increased levels of pro-inflammatory cytokines, including IL-1β, IFN-γ and TNF-α, 8 weeks following AAV-A53T α-Syn administration into the SN.

The current results extend the information regarding the early microglial response to α-Syn by quantifying the morphological changes that occur in striatal microglia consequent to over-expression of A53T α-Syn in the SN and the extent to which these changes in microglial morphology can be modified by GM1 ganglioside administration. Microglial process length per cell and number of endpoints per cell, measures of extent of microglial ramification (Young and Morrison, 2018), were significantly decreased in striatum and both measures were normalized in animals that received four weeks of GM1 administration. Lower fractal dimension and lacunarity indices indicate decreased branch complexity and decreased heterogeneity, respectively in α-Syn/saline-treated animals. Increased density and decreased cell perimeter measures indicated that microglia in these animals had a more compact shape, consistent with activation, compared with microglia on the

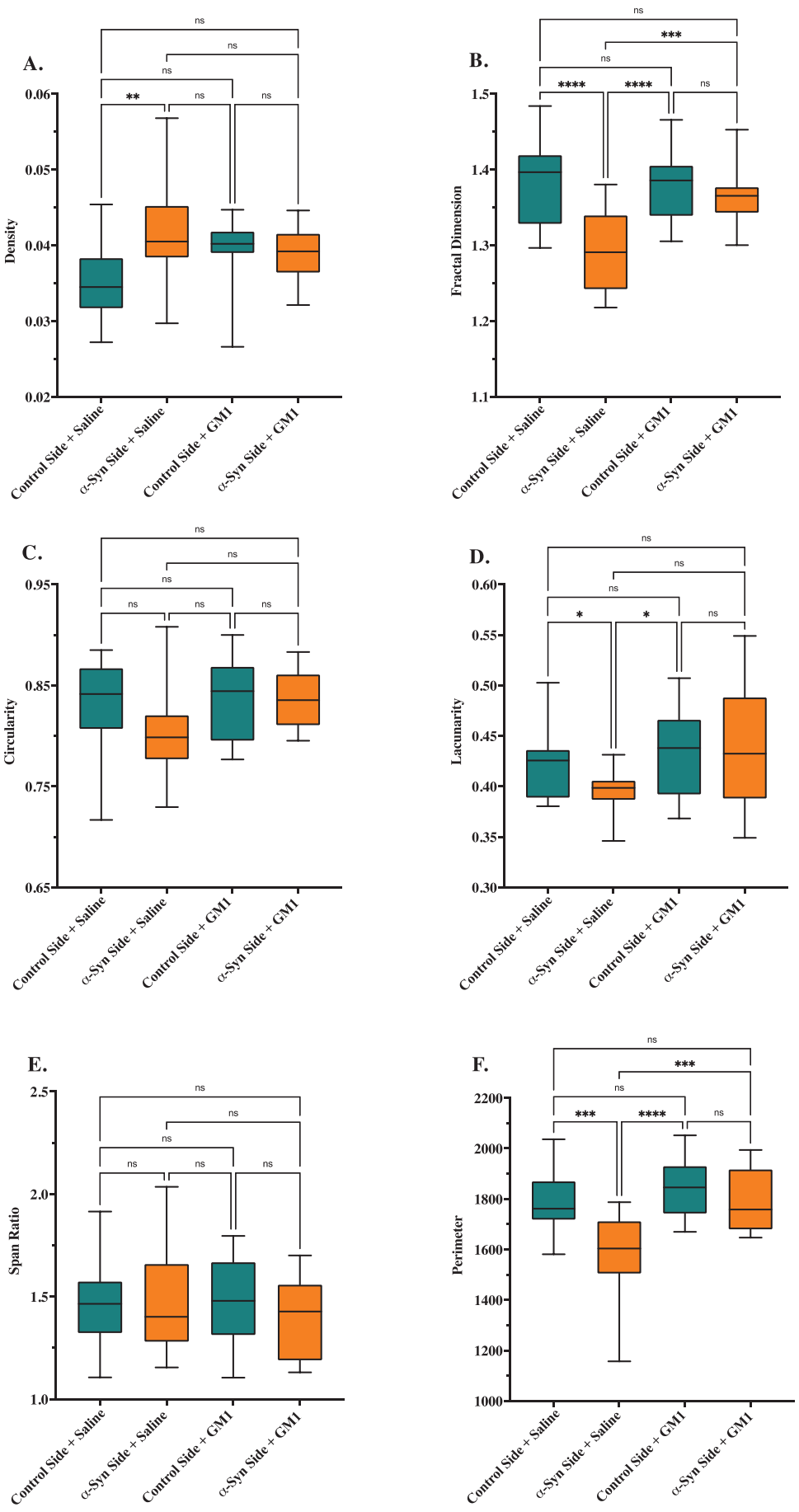

Fig. 7. Changes in morphological parameters of density, fractal dimension, lacunarity, and cell perimeter are consistent with microglial activation in response to α-synuclein (α-Syn) toxicity and a reversal of this response in animals treated with GM1 ganglioside for 4 weeks. In saline-treated animals, activation of microglia was evidenced by higher density on the α-Syn side of the brain vs. the control, non-injected side (A), which together with lower cell perimeter (F), implies a more compact shape. These parameters were not significantly different on the control and α-Syn sides in GM1-treated animals. Activation of microglia in saline-treated animals was also implied by the lower fractal dimension (B) and lower lacunarity (D) on the α-Syn vs. control sides of the brain, indicating decreased branch complexity and heterogeneity, respectively. These parameters were not significantly different on the control and α-Syn sides in GM1-treated animals. (*$P < 0.05$, **$P < 0.01$, ***$P < 0.001$, ****$P < 0.0001$, for the indicated comparisons. Data are presented as box and whisker graphs (Min to Max) from N = 5 animals per treatment group (saline, GM1) and N = 3 randomly selected cells from each side of the striatum from each animal).

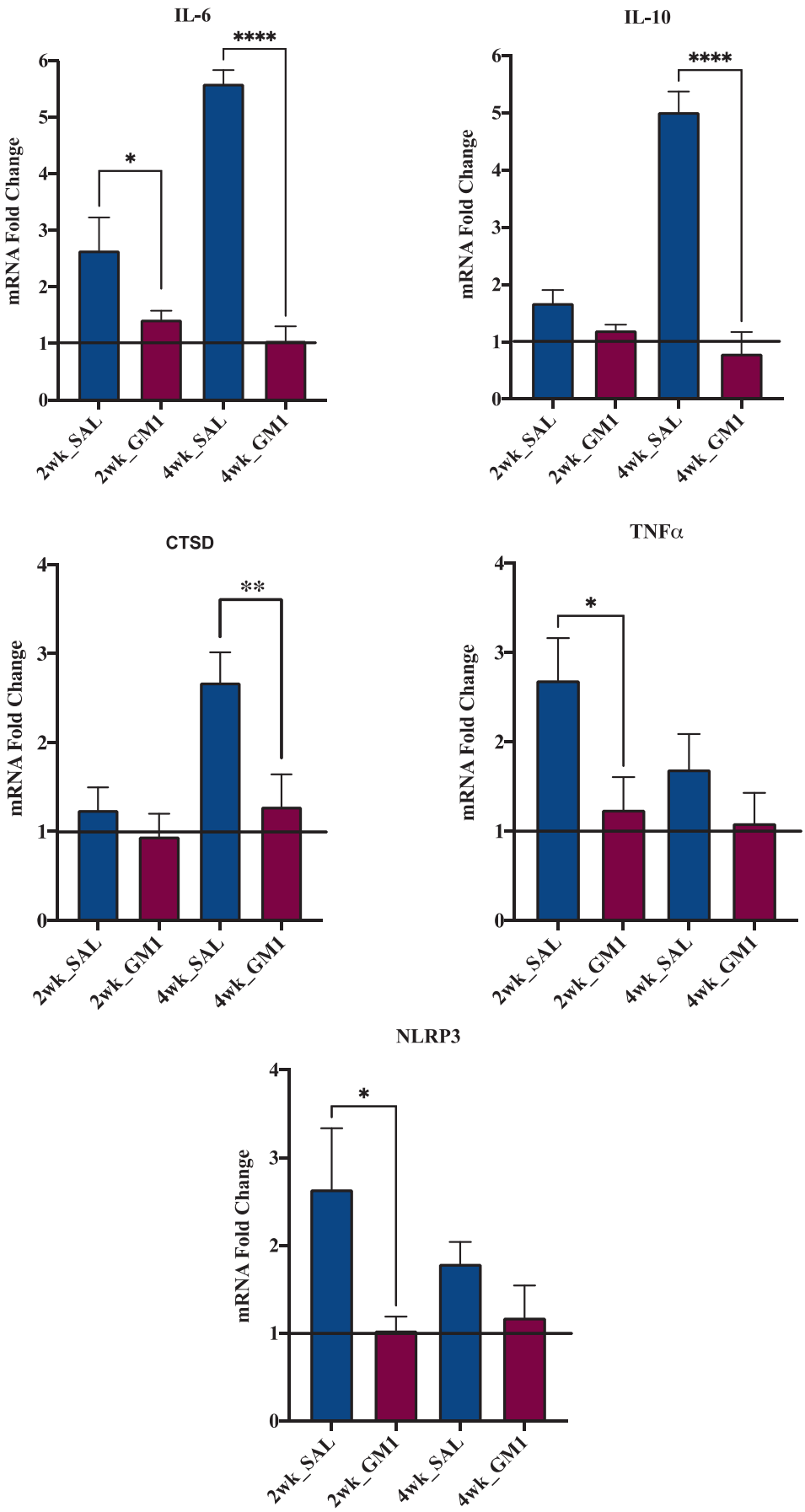

Fig. 8. Upregulation of expression of neuroinflammation-related genes in response to α-synuclein overexpression in saline treated animals but not in GM1-treated animals. Expression of interleukin-6 (IL-6), cathepsin D (CTSD), and interleukin-10 (IL-10) were significantly upregulated at four weeks after AAV-A53T α-synuclein injection into the SN on the left side (compared with expression on the right, control side) in saline-treated animals but not in GM1-treated animals. Expression of tumor necrosis factor alpha (TNFα) and NLR family pyrin domain containing 3 (NLRP3) inflammasome were significantly increased in saline-treated animals but not in GM1-treated animals at two weeks post surgery and while similar trends were observed at 4 weeks, these comparisons were not statistically significant. Data are presented as mean fold change (±SEM) in left/right ratios from N = 8 (2 week saline and 4 week saline) and N = 9 (2 week GM1 and 4 week GM1). $*P < 0.05$, $**P < 0.01$, $****P < 0.0001$, for the indicated comparisons.

control side of the brain. All of these measures indicative of microglial activation and neuroinflammation were reversed or normalized in animals treated with GM1 ganglioside. These findings are consistent with a recent report that gangliosides, and in particular GM1, plays an important role in modulating microglial functions and responses to pro-inflammatory signals and exerts an anti-inflammatory effect (Galleguillos et al., 2022).

Our results using the AAV-A53T-α-Syn model also showed that α-Syn overexpression results in both microglial activation and upregulation of pro-inflammatory molecules, consistent with what has been described by others (Chung et al., 2009; Su et al., 2009; Su et al., 2008). Importantly, we show here that treatment with GM1 ganglioside can at least partially counteract these adverse responses to potentially toxic α-Syn accumulation. We found that IL-6, IL-10, CTSD, TNFα, and NLRP3 gene expression was significantly increased in the α-Syn-injected SN compared to the control, non-injected SN and that expression was normalized in GM1-treated animals. There is evidence for α-Syn-mediated activation of the NLRP3 inflammasome in the SN in PD as well in animal PD models, contributing to pro-inflammatory responses and DAergic neuron degeneration (Gordon et al., 2018). Incubation with α-Syn produced significant TNFα release from microglia *in vitro* and injection of α-Syn into the SN led to upregulation of gene expression of pro-inflammatory cytokines IL-1β, IL-6 and TNFα by 24 h after injection (Couch et al., 2011). We have likewise observed an upregulation of gene expression of IL-6 and TNFα in the SN four weeks after AAV-A53T-α-Syn injection and this was not seen in GM1-treated animals. Recently Galleguillos et al. (2022) reported that GM1 ganglioside administration decreased inflammatory microglial responses *in vivo* and *in vitro*, with GM1 inhibiting lipopolysaccharide (LPS)-induced IL-1β and TNFα gene upregulation and decreasing IL-1β, IL-6 and TNFα cytokine levels. Production of IL-10, an anti-inflammatory cytokine, is an important mechanism to counteract damage driven by excessive inflammation (Lobo-Silva et al., 2016), however, the action of IL-10 may vary in different disease states. In Alzheimer's disease models for example, IL-10 had a detrimental effect on amyloid accumulation and it has been suggested that inhibiting the actions of key anti-inflammatory cytokines, such as IL-10, may allow the brain to return to a physiologically balanced state with a potentially therapeutic effect (Lobo-Silva et al., 2016; Guillot-Sestier et al., 2015). IL-10 signaling also upregulated microgliosis, enhanced neurodegeneration, and decreased survival in A53T α-Syn transgenic mice (Cockey et al., 2021). In the present study, we found a significant upregulation of 1L-10 gene expression in AAV-A53T-α-Syn/saline treated animals but not in AAV-A53T-α-Syn/GM1-treated animals. The ability of GM1 administration to counter a potentially detrimental IL-10 response is consistent with the effects of GM1 on microglial morphology and neuroprotection in this model. The lack of change observed in gene expression of other inflammatory-related genes (i.e., IL-1β, Nurr1, PTGS2, or NOS2) in our AAV-A53T-α-Syn/saline animals was surprising and the reasons for this are not clear at this time, but may potentially be related to the tissue analyzed (SN versus striatum) and/or the time at which the tissues were examined (i.e., 2–4 weeks after AAV-A53T-α-Syn injection). Also, although the current study did not employ an empty vector control group, we don't believe that this impacts the results reported. In our previous study of the effects of GM1 administration in the rat AAV-A53T-synuclein model (Schneider et al., 2019) we employed an empty vector control and found that the empty vector produced no pathological response and had no effect on behavior, striatal DA and metabolite levels, or on SN cell counts. Using the same AAV-A53T-α-Syn vector that we have used in the prior study and in the current study, Chung et al. (2009) also showed that AAV-A53T-α-Syn vector administration to the SN resulted in an early appearing microglial activation and neuroinflammatory response in the striatum and reported no evidence of microglial activation or any increases in neuroinflammatory markers in animals that received control vector injections.

In summary, we previously showed in the AAV-A53T α-Syn model that GM1 administration was neuroprotective/neurorestorative and that effects were associated with decreased aggregation of α-Syn and decreased α-Syn phosphorylation. In addition to decreasing the accumulation of toxic forms of α-Syn, the present data show that GM1 treatment also appears to modulate microglial morphology and neuroinflammatory responses to potentially toxic α-Syn, further contributing to its neuroprotective/neurorestorative effects. The inhibition of microglial activation and potentially damaging neuroinflammation by GM1 ganglioside administration may be among the many factors that contribute to the neuroprotective/neurorestorative effects of GM1 in the AAV-A53T α-Syn PD model (Schneider et al., 2019) and possibly in other PD models (Hadaczek et al., 2015). These mechanisms of action of GM1 may also potentially contribute to a previously reported disease-modifying effect of GM1 observed in human PD (Schneider et al., 2013).

Supplementary data to this article can be found online at https://doi.org/10.1016/j.mcn.2022.103729.

CRediT authorship contribution statement

Jay S. Schneider: Conceptualization, Methodology, Investigation, Formal analysis, Supervision, Writing – original draft, Writing – review & editing. **Garima Singh:** Conceptualization, Methodology, Investigation, Formal analysis, Writing – review & editing. **Courtney K. Williams:** Methodology, Investigation, Writing – review & editing. **Vikrant Singh:** Conceptualization, Methodology, Investigation, Formal analysis, Writing – review & editing.

Declaration of competing interest

For author J. Schneider, this research has been funded by Qilu Pharmaceutical Co., Ltd., a company with a commercial interest in GM1 ganglioside. The funder had no role in the conceptualization, design, data collection, analysis, decision to publish, or preparation of this manuscript. J. Schneider is a named inventor on a patent entitled, “Gene Therapies for Neurodegenerative Disorders Targeting Ganglioside Biosynthetic Pathways”, US Patent 10,874,749, assigned to Thomas Jefferson University.

For authors C. Williams, V. Singh, and G. Singh, no competing interests.

Acknowledgements

This research was funded by a grant from Qilu Pharmaceutical, Co., Ltd.

References

Chung, C.Y., Koprich, J.B., Siddiqi, H., Isacson, O., 2009. Dynamic changes in presynaptic and axonal transport proteins combined with striatal neuroinflammation precede dopaminergic neuronal loss in a rat model of AAV alpha-synucleinopathy. J. Neurosci. 29, 3365–3373.

Cockey, S.G., McFarland, K.N., Koller, E.J., Brooks, M.M.T., Gonzalez De La Cruz, E., Cruz, P.E., Ceballos-Diaz, C., Rosario, A.M., Levites, Y.R., Borchelt, D.R., Golde, T.E., Giasson, B.I., Chakrabarty, P., 2021. Il-10 signaling reduces survival in mouse models of synucleinopathy. NPJ Parkinsons Dis. 7, 30.

Couch, Y., Alvarez-Erviti, L., Sibson, N.R., Wood, M.J., Anthony, D.C., 2011. The acute inflammatory response to intranigral alpha-synuclein differs significantly from intranigral lipopolysaccharide and is exacerbated by peripheral inflammation. J. Neuroinflammation 8, 166.

Du, Y., Ma, Z., Lin, S., Dodel, R.C., Gao, F., Bales, K.R., Triarhou, L.C., Chernet, E., Perry, K.W., Nelson, D.L., Luecke, S., Phebus, L.A., Bymaster, F.P., Paul, S.M., 2001. Minocycline prevents nigrostriatal dopaminergic neurodegeneration in the MPTP model of Parkinson's disease. Proc. Natl. Acad. Sci. U. S. A. 98, 14669–14674.

Fernandez-Arjona, M.D.M., Grondona, J.M., Granados-Duran, P., Fernandez-Llebrez, P., Lopez-Avalos, M.D., 2017. Microglia morphological categorization in a rat model of neuroinflammation by hierarchical cluster and principal components analysis. Front. Cell. Neurosci. 11, 235.

Ferreira, M., Massano, J., 2017. An updated review of Parkinson's disease genetics and clinicopathological correlations. Acta Neurol. Scand. 135, 273–284.

Furuya, T., Hayakawa, H., Yamada, M., Yoshimi, K., Hisahara, S., Miura, M., Mizuno, Y., Mochizuki, H., 2004. Caspase-11 mediates inflammatory dopaminergic cell death in

the 1-methyl-4-phenyl-1,2,3,6-tetrahydropyridine mouse model of Parkinson's disease. J. Neurosci. 24, 1865–1872.
Galleguillos, D., Wang, Q., Steinberg, N., Zaidi, A., Shrivastava, G., Dhami, K., Daskhan, G.C., Schmidt, E.N., Dworsky-Fried, Z., Giuliani, F., Churchward, M., Power, C., Todd, K., Taylor, A., Macauley, M.S., Sipione, S., 2022. Anti-inflammatory role of GM1 and other gangliosides on microglia. J. Neuroinflammation 19, 9.
Gerhard, A., Pavese, N., Hotton, G., Turkheimer, F., Es, M., Hammers, A., Eggert, K., Oertel, W., Banati, R.B., Brooks, D.J., 2006. In vivo imaging of microglial activation with [11C](R)-PK11195 PET in idiopathic Parkinson's disease. Neurobiol. Dis. 21, 404–412.
Gordon, R., Albornoz, E.A., Christie, D.C., Langley, M.R., Kumar, V., Mantovani, S., Robertson, A.A.B., Butler, M.S., Rowe, D.B., O'Neill, L.A., Kanthasamy, A.G., Schroder, K., Cooper, M.A., Woodruff, T.M., 2018. Inflammasome inhibition prevents alpha-synuclein pathology and dopaminergic neurodegeneration in mice. Sci. Transl. Med. 10.
Guillot-Sestier, M.V., Doty, K.R., Gate, D., Rodriguez Jr., J., Leung, B.P., Rezai-Zadeh, K., Town, T., 2015. Il10 deficiency rebalances innate immunity to mitigate Alzheimer-like pathology. Neuron 85, 534–548.
Hadaczek, P., Wu, G., Sharma, N., Ciesielska, A., Bankiewicz, K., Davidow, A.L., Lu, Z.H., Forsayeth, J., Ledeen, R.W., 2015. GDNF signaling implemented by GM1 ganglioside; failure in Parkinson's disease and GM1-deficient murine model. Exp. Neurol. 263, 177–189.
He, Y., Appel, S., Le, W., 2001. Minocycline inhibits microglial activation and protects nigral cells after 6-hydroxydopamine injection into mouse striatum. Brain Res. 909, 187–193.
Ho, S.L., McCann, K.P., Bennett, P., Kapadi, A.L., Waring, R.H., Ramsden, D.B., Williams, A.C., 1996. The molecular biology of xenobiotic enzymes and the predisposition to idiopathic Parkinson's disease. Adv. Neurol. 69, 53–60.
Hung, A.Y., Schwarzschild, M.A., 2020. Approaches to disease modification for Parkinson's disease: clinical trials and lessons learned. Neurotherapeutics 17, 1393–1405.
Jenner, P., 1991. Oxidative stress as a cause of Parkinson's disease. Acta Neurol. Scand. Suppl. 136, 6–15.
Karperien, A., Ahammer, H., Jelinek, H.F., 2013. Quantitating the subtleties of microglial morphology with fractal analysis. Front. Cell. Neurosci. 7, 3.
Koprich, J.B., Johnston, T.H., Huot, P., Reyes, M.G., Espinosa, M., Brotchie, J.M., 2011. Progressive neurodegeneration or endogenous compensation in an animal model of Parkinson's disease produced by decreasing doses of alpha-synuclein. PLoS One 6, e17698.
Kurkowska-Jastrzebska, I., Wronska, A., Kohutnicka, M., Czlonkowski, A., Czlonkowska, A., 1999. The inflammatory reaction following 1-methyl-4-phenyl-1,2,3, 6-tetrahydropyridine intoxication in mouse. Exp. Neurol. 156, 50–61.
Langston, J.W., Forno, L.S., Tetrud, J., Reeves, A.G., Kaplan, J.A., Karluk, D., 1999. Evidence of active nerve cell degeneration in the substantia nigra of humans years after 1-methyl-4-phenyl-1,2,3,6-tetrahydropyridine exposure. Ann. Neurol. 46, 598–605.
LaVoie, M.J., Card, J.P., Hastings, T.G., 2004. Microglial activation precedes dopamine terminal pathology in methamphetamine-induced neurotoxicity. Exp. Neurol. 187, 47–57.
Ledeen, R.W., Wu, G., 2015. The multi-tasked life of GM1 ganglioside, a true factotum of nature. Trends Biochem. Sci. 40, 407–418.
Lobo-Silva, D., Carriche, G.M., Castro, A.G., Roque, S., Saraiva, M., 2016. Balancing the immune response in the brain: IL-10 and its regulation. J. Neuroinflammation 13, 297.
McGeer, P.L., Itagaki, S., Boyes, B.E., McGeer, E.G., 1988. Reactive microglia are positive for HLA-DR in the substantia nigra of Parkinson's and Alzheimer's disease brains. Neurology 38, 1285–1291.
Mogi, M., Harada, M., Kondo, T., Riederer, P., Inagaki, H., Minami, M., Nagatsu, T., 1994. Interleukin-1 beta, interleukin-6, epidermal growth factor and transforming growth factor-alpha are elevated in the brain from parkinsonian patients. Neurosci. Lett. 180, 147–150.
Morrison, H., Young, K., Qureshi, M., Rowe, R.K., Lifshitz, J., 2017. Quantitative microglia analyses reveal diverse morphologic responses in the rat cortex after diffuse brain injury. Sci. Rep. 7, 13211.
Ostrerova-Golts, N., Petrucelli, L., Hardy, J., Lee, J.M., Farer, M., Wolozin, B., 2000. The A53T alpha-synuclein mutation increases iron-dependent aggregation and toxicity. J. Neurosci. 20, 6048–6054.
Ouchi, Y., Yoshikawa, E., Sekine, Y., Futatsubashi, M., Kanno, T., Ogusu, T., Torizuka, T., 2005. Microglial activation and dopamine terminal loss in early Parkinson's disease. Ann. Neurol. 57, 168–175.
Park, J.Y., Kim, K.S., Lee, S.B., Ryu, J.S., Chung, K.C., Choo, Y.K., Jou, I., Kim, J., Park, S. M., 2009. On the mechanism of internalization of alpha-synuclein into microglia: roles of ganglioside GM1 and lipid raft. J. Neurochem. 110, 400–411.
Rocha, E.M., De Miranda, B., Sanders, L.H., 2018. Alpha-synuclein: pathology, mitochondrial dysfunction and neuroinflammation in Parkinson's disease. Neurobiol. Dis. 109, 249–257.
Sanchez-Guajardo, V., Febbraro, F., Kirik, D., Romero-Ramos, M., 2010. Microglia acquire distinct activation profiles depending on the degree of alpha-synuclein neuropathology in a rAAV based model of Parkinson's disease. PLoS One 5, e8784.
Schapira, A.H., Cooper, J.M., Dexter, D., Clark, J.B., Jenner, P., Marsden, C.D., 1990. Mitochondrial complex I deficiency in Parkinson's disease. J. Neurochem. 54, 823–827.
Schapira, A.H., Gu, M., Taanman, J.W., Tabrizi, S.J., Seaton, T., Cleeter, M., Cooper, J. M., 1998. Mitochondria in the etiology and pathogenesis of Parkinson's disease. Ann. Neurol. 44, S89–S98.
Schneider, J.S., 2021. A critical role for GM1 ganglioside in the pathophysiology and potential treatment of Parkinson's disease. Glycoconj. J. 39, 13–26.
Schneider, J.S., Aras, R., Williams, C.K., Koprich, J.B., Brotchie, J.M., Singh, V., 2019. GM1 ganglioside modifies alpha-synuclein toxicity and is neuroprotective in a rat alpha-synuclein model of Parkinson's disease. Sci. Rep. 9, 8362.
Schneider, J.S., Gollomp, S.M., Sendek, S., Colcher, A., Cambi, F., Du, W., 2013. A randomized, controlled, delayed start trial of GM1 ganglioside in treated Parkinson's disease patients. J. Neurol. Sci. 324, 140–148.
Su, X., Federoff, H.J., Maguire-Zeiss, K.A., 2009. Mutant alpha-synuclein overexpression mediates early proinflammatory activity. Neurotox. Res. 16, 238–254.
Su, X., Maguire-Zeiss, K.A., Giuliano, R., Prifti, L., Venkatesh, K., Federoff, H.J., 2008. Synuclein activates microglia in a model of Parkinson's disease. Neurobiol. Aging 29, 1690–1701.
Tomac, A., Lindqvist, E., Lin, L.F., Ogren, S.O., Young, D., Hoffer, B.J., Olson, L., 1995. Protection and repair of the nigrostriatal dopaminergic system by GDNF in vivo. Nature 373, 335–339.
Wang, S., Chu, C.H., Guo, M., Jiang, L., Nie, H., Zhang, W., Wilson, B., Yang, L., Stewart, T., Hong, J.S., Zhang, J., 2016. Identification of a specific alpha-synuclein peptide (alpha-syn 29–40) capable of eliciting microglial superoxide production to damage dopaminergic neurons. J. Neuroinflammation 13, 158.
Wu, D.C., Jackson-Lewis, V., Vila, M., Tieu, K., Teismann, P., Vadseth, C., Choi, D.K., Ischiropoulos, H., Przedborski, S., 2002. Blockade of microglial activation is neuroprotective in the 1-methyl-4-phenyl-1,2,3,6-tetrahydropyridine mouse model of Parkinson disease. J. Neurosci. 22, 1763–1771.
Young, K., Morrison, H., 2018. Quantifying microglia morphology from photomicrographs of immunohistochemistry prepared tissue using ImageJ. JoVe (J. Vis. Exp.) 136, e57648.
Zhang, Q.S., Heng, Y., Yuan, Y.H., Chen, N.H., 2017. Pathological alpha-synuclein exacerbates the progression of Parkinson's disease through microglial activation. Toxicol. Lett. 265, 30–37.
Zhang, W., Dallas, S., Zhang, D., Guo, J.P., Pang, H., Wilson, B., Miller, D.S., Chen, B., Zhang, W., McGeer, P.L., Hong, J.S., Zhang, J., 2007. Microglial PHOX and mac-1 are essential to the enhanced dopaminergic neurodegeneration elicited by A30P and A53T mutant alpha-synuclein. Glia 55, 1178–1188.
Zhang, W., Wang, T., Pei, Z., Miller, D.S., Wu, X., Block, M.L., Wilson, B., Zhang, W., Zhou, Y., Hong, J.S., Zhang, J., 2005. Aggregated alpha-synuclein activates microglia: a process leading to disease progression in Parkinson's disease. FASEB J. 19, 533–542.